



Orbital Debris Quarterly News

Volume 11, Issue 4

October 2007

Inside...

Another Collision Avoidance Maneuver Made by NASA Satellite.....	2
Two Minor Satellite Fragmentations Identified in the Third Quarter.....	2
ISS Zarya Control Module Impact Damage.....	3
Three New Satellite Impact Tests.....	4
A Preliminary Active Debris Removal Study.....	6
Abstracts from the NASA Orbital Debris Program Office.....	7
Space Missions and Orbital Box Score.....	12



A publication of
The NASA Orbital Debris Program Office

New NASA Procedural Requirement and Technical Standard for Limiting Orbital Debris Generation

On 17 August 2007, NASA's Chief Safety and Mission Assurance Officer, Bryan O'Connor, signed NASA Procedural Requirements (NPR) 8715.6, the latest revision in NASA's 15-year-old policy designed to curtail the growth of the orbital debris population. On 28 August 2007, the NASA Technical Standard (NS) 8719.14 was also signed by Bryan O'Connor, updating the aging NASA Safety Standard 1740.14, *Guidelines and Assessment Procedures for Limiting Orbital Debris*, issued in 1995.

NPR 8715.6 recognizes the ongoing importance of orbital debris mitigation, both nationally and internationally, and a need to expand the responsibilities of various organizations within NASA. Fourteen organizations or positions within NASA are now assigned explicit orbital debris mitigation duties by the NPR, in contrast to only ten organizations or positions cited in the previous NASA Policy Directive (NPD 8710.3B), and only four in the policy before that one.

The NPR provides requirements to implement NASA's policy for limiting orbital debris generation per the U.S. National Space Policy of 2006, Section 11. In conjunction with the related NASA standard, the NPR is consistent with the United Nations Committee on the Peaceful Uses of Outer Space (UNCOPUOS) Space Debris Mitigation Guidelines, as well as Inter-Agency Space Debris Coordination Committee (IADC) Space Debris Mitigation Guidelines.

As outlined in section 1.3.11 of the NPR, the NASA Orbital Debris Program Office shall:

1. Develop, maintain, and update the orbital debris environment models to support this NPR.
2. Assist NASA mission program/project managers in technical orbital debris assessments.
3. Provide assistance to the Department of Defense and other U.S. Government departments

and organizations on matters related to the characterization of the orbital debris environment and the application of orbital debris mitigation measures and policies for NASA space missions.

4. Participate in the determination, adoption, and use of international orbital debris mitigation guidelines through international forums such as the UNCOUOS, the IADC, and the International Organization for Standardization (ISO).

5. Maintain a list of predicted reentry dates for NASA spacecraft and their associated orbital stages and notify the Office of Safety and Mission Assurance at least 60 days prior to their reentry.

Approved by NASA Headquarters and NASA Centers, NS 8719.14 provides uniform engineering and technical requirements for processes, procedures, practices, and methods for NASA programs and projects to adhere to orbital debris requirements.

NS 8719.14 requires NASA projects to assess compliance in the following areas:

1. Debris Released During Normal Operations
2. Debris Released by Explosions and Intentional Breakups
3. Debris Generated by On-Orbit Collisions
4. Postmission Disposal of Space Structures
5. Survival of Debris from the Postmission Disposal Atmospheric Reentry Option
6. Tether Missions

The Standard reflects significant improvements in both the technical foundation of the standard and assessment process, as well as addressing new areas of debris mitigation, such as tethers, the

continued on page 2

NASA Procedural Requirement

continued from page 1

Moon, Mars, and Lagrange points. Where appropriate, minor changes were incorporated to ensure that the Standard is consistent with the latest national and international orbital debris mitigation guidelines.

In support of the new Standard, the NASA Orbital Debris Program Office will

soon release an updated version of the Debris Assessment Software (DAS) to assist projects in the technical aspects of assessing compliance with the requirements. The software release will be called DAS 2.0.

A copy of the NPR 8715.6 and NS 8719.14 can be obtained via the

Orbital Debris Program Office website at <www.orbitaldebris.jsc.nasa.gov> ♦

Another Collision Avoidance Maneuver Made by NASA Satellite

Less than two weeks after NASA's Terra spacecraft had to execute a collision-avoidance maneuver to evade a piece of debris from the January Chinese ASAT test (ODQN, April 2007, p. 2), a sister NASA satellite in the multinational Earth Observation System (EOS) constellation was forced to dodge a close encounter with another resident space object.

NASA's Cloudsat spacecraft (International Designator 2006-016A, U.S. Satellite Number 29107) was launched in April 2006, and circles the Earth at a mean altitude of 705 km, the same orbit type as Terra. It flies in close

proximity with the Aura, Aqua, CALIPSO, and PARASOL satellites in the so-called "A-Train Formation." Each EOS satellite is routinely screened for possible close approaches with other resident space objects, including both orbital debris and operational spacecraft. In early July 2007, such an analysis indicated that Cloudsat would come close to the Iranian Sinah 1 spacecraft (International Designator 2005-043D, U.S. Satellite Number 28893) on 6 July. Sinah 1 is a small Russian-built spacecraft with a mean orbital altitude about 10 km below that of Cloudsat, but which does

intersect the orbit of Cloudsat near apogee.

Refinements of the conjunction assessment indicated a miss distance on the order of only 100 m. Given this predicted close approach and inherent uncertainties, a decision was made to maneuver Cloudsat on 4 July. The post-maneuver orbit increased the miss distance to about 4 km. On 7 July Cloudsat was maneuvered again to return the spacecraft to its tightly controlled ground-track and position within the A-Train. ♦

Two Minor Satellite Fragmentations Identified in the Third Quarter

After five satellite breakups in the first two months of 2007 (ODQN, April 2007, pp. 2-3), no significant fragmentations have since been detected. In the third quarter of the year, only two minor fragmentations were identified by the U.S. Space Surveillance Network (SSN).

On 25 July, the second stage of the Japanese H-2A rocket body (International Designator 2006-037B, U.S. Satellite Number 29394), which placed the IGS-3A spacecraft into orbit in September 2006, experienced a second debris generation event. The first release of debris, totaling less than 20 objects, occurred on 28 December 2006 (ODQN, January 2007, pp. 2-3). The July incident, when the rocket body was in an orbit of approximately 430 km by 485 km, produced an estimated 15 new debris, although only nine fragments were officially cataloged (U.S. Satellite Numbers 32009-32017). All tracked debris, except one, exhibited high area-to-mass

ratios and had reentered by the end of August.

The two fragmentation events for this stage bear a resemblance to two minor fragmentations of another Japanese upper stage launched in 2006. The second stage of the H-2A, which launched the ALOS-1 spacecraft in January 2006, experienced two debris generation events in August of that year (ODQN, October 2006, p. 1). The cause of all four debris releases remains under investigation by Japanese specialists.

The separation of a single piece of debris from Canada's ISIS 1 spacecraft (International Designator 1969-009A, U.S. Satellite Number 3669) on 24 May 2007 was confirmed in the third quarter. At the time of the event, ISIS 1 was in an orbit of 580 km by 3455 km at an inclination of 88.5 degrees. The new fragment, which was released with very low velocity, was cataloged as U.S. Satellite Number 31999. The roughly ellipsoidal, 38-year-old

spacecraft was covered with solar cells and nine protruding wire antennae. The nature of the released fragment is currently unknown.

Knowledge concerning the extent of the orbital debris cloud from the January 2007 destruction of the Fengyun-1C meteorological satellite by the impact of a Chinese anti-satellite device continues to improve. By the end of September, the total number of cataloged debris had reached 2087. However, the total number of debris being tracked by the US SSN, widely distributed in orbits between 200 km to 4000 km, exceeded 2500. Unfortunately the orbital decay of these large debris (greater than approximately 10 cm in diameter) remains very slow: on average only two reentries per month. A recent analysis by the NASA Orbital Debris Program Office indicates that the majority of the cataloged debris will stay in orbit for decades, some for more than a century. ♦

Visit the NASA Orbital Debris Program Office Website

www.orbitaldebris.jsc.nasa.gov

PROJECT REVIEWS

ISS Zarya Control Module Impact Damage

E. CHRISTIANSEN, T. PRIOR, F. LYONS, D. LEAR, AND J. HYDE

During Russian-Segment Extravehicular Activity Number 19 on the International Space Station in June 2007, the crew reported damage to the exterior thermal blanket covering the Zarya Control Module (FGB) compressor unit, describing it as appearing like a “bullet hit.” A photograph of the damage is shown in Figure 1, and the location of the compressor on the forward end of the FGB is illustrated in Figure 2. The tear in the thermal blanket outer cover was approximately 6.7 cm long by 3.3 cm wide. A smaller hole in the underlying layers of the multi-layer insulation blanket measured 1.0 cm x 0.85 cm.

Because of the shape of the damage, it was thought that the damage was caused by a highly oblique impact from a micro-meteoroid or orbital debris particle. Hypervelocity impact tests were conducted at NASA White Sands Test Facility on realistic samples of the micro-meteoroid and orbital debris (MMOD) shielding covering the compressor area to determine a possible size of the impacting particle and to determine the characteristics of the damage if this particle impacted at another (less oblique) impact angle. The JSC Hypervelocity Impact Technology Facility (HITF) developed the test plan and built the test articles using a spare Russian thermal blanket that was available from a previous test program for the hypervelocity impact tests. A cross-section of the MMOD shielding in this area of the FGB is shown in Figure 3 and is composed of the exterior thermal blanket, steel mesh, fiberglass cloth, aluminum honeycomb sandwich, a steel casing protecting the compressor components, and the aluminum pressure shell of the FGB.

Figure 4 illustrates damage to the exterior thermal blanket from one of the hypervelocity impact tests. In this test (HITF-7310), a 0.2 cm-diameter, aluminum spherical projectile impacted the target at 6.78 km/s with an impact angle 70° from a normal to the target. A 4.8 cm x 2.3 cm hole was generated in the exterior fabric cover from this test, which is slightly smaller than the actual damage (6.7 cm x 3.3 cm). The front facesheet of the honeycomb was nearly penetrated in this test and the back facesheet was slightly bulged, but not penetrated. In another test, with a 0.3 cm-diameter, aluminum projectile at the same 70° impact angle and similar velocity,

the hole in the exterior fabric cover was 7.8 cm x 3.9 cm, or slightly greater than the actual damage. Based on these test results, we believe the likely particle size causing the damage was between 0.2 cm and 0.3 cm in size, impacting at a highly oblique angle. We also believe, based on the test results, that the honeycomb panel is likely damaged but not completely penetrated, that no damage occurred to

continued on page 4



Figure 1. Damage to FGB thermal blanket observed by RS EVA-19 crew. Note, each square on the exterior fabric of the thermal blanket is ~ 1 cm x 1 cm. The tear in the exterior fabric cover is 6.7 cm x 3.3 cm and the hole in the underlying thermal blanket layers is 1.0 cm x 0.85 cm.

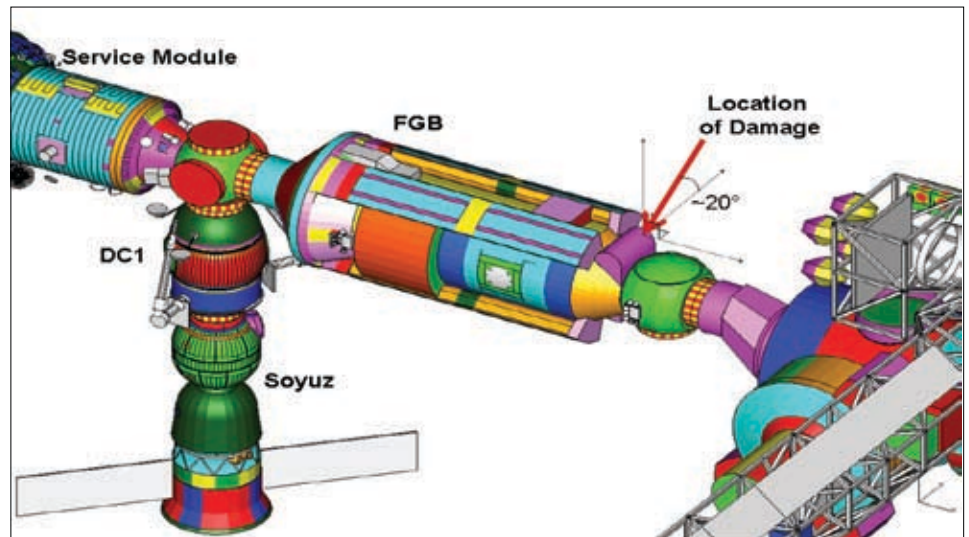


Figure 2. Location of impact damage on FGB compressor (indicated by red arrow).

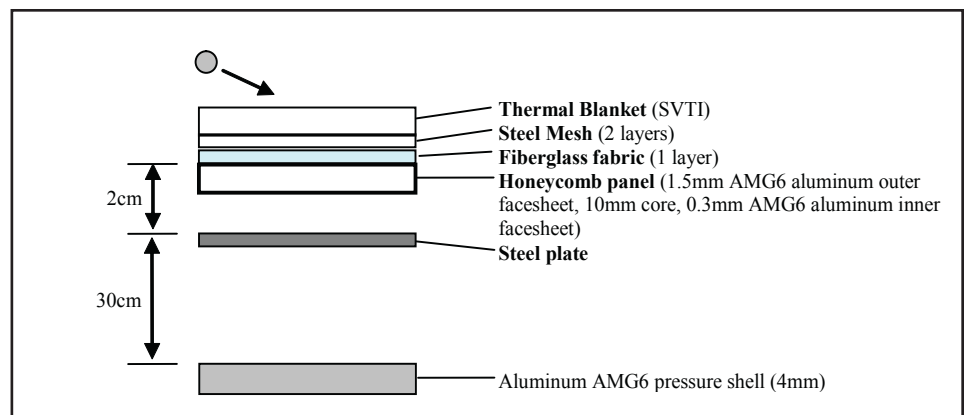


Figure 3. Cross-section of MMOD shielding in area of FGB compressors.

ISS Zarya Control Module

continued from page 3

the compressor housing or other equipment in this area of the module, and that no damage occurred to the pressure shell of the FGB. Figure 5 compares the 0.2 cm- to 0.3 cm-size particle causing the FGB damage with the particle sizes predicted to completely penetrate the shielding and pressure shell in the FGB compressor area. It was also noted that the hole size in the underlying thermal blanket layers appears larger in the ground tests compared to the actual damage, indicating the actual impact velocity may have been lower than the test speeds of ~6.78 km/s. Because there was a very limited amount of thermal blanket available for these tests, additional testing at lower impact speeds was not performed.

Another test, HITF-7311, was performed with the same size particle (0.2 cm diameter) that caused the large exterior tear in the thermal blanket illustrated in Figure 4, but at a 0° impact angle (i.e., normal to the target). The purpose of this test was to determine how the depth

of penetration and size of damage on the exterior blanket changes at a different impact angle. Figure 6 illustrates the consequence of this impact. The hole in the exterior thermal blanket was 0.3 cm in size (much smaller than at the 70° impact angle), but the honeycomb panel was completely penetrated and the compressor housing damaged. It is interesting to note that a very oblique impact may cause a considerable amount of visible impact damage, but may not penetrate very deep into the shielding; whereas, smaller visible damage could

correspond to internal damage that penetrates much deeper into the shielding and underlying equipment. ♦

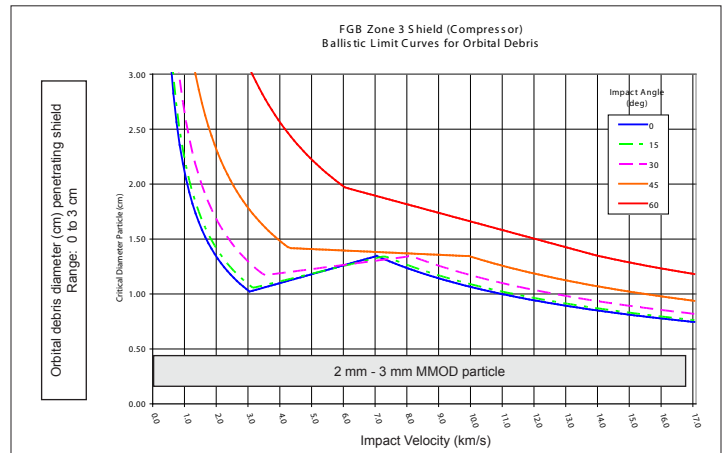


Figure 5. Diameter of aluminum orbital debris particle as a function of impact angle (colored lines) and impact velocity for the compressor region of the FGB. Impacts on or above the lines are expected to fail the shield (creating a hole in the pressure shell). Note that 0.2 cm - 0.3 cm (2-3 mm) diameter particles are not expected to penetrate through the shielding and pressure shell.

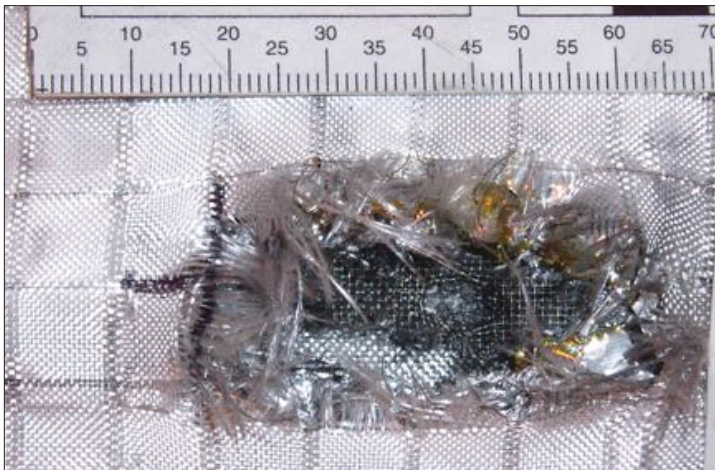


Figure 4. Damage to exterior thermal blanket on a target mockup from ground test number HITF-7310. The projectile was a 0.2 cm-diameter aluminum (2017-T4 alloy) sphere, impact speed 6.78 km/s, impact angle 70 deg from normal. The scale at the top of the photo is in millimeters.

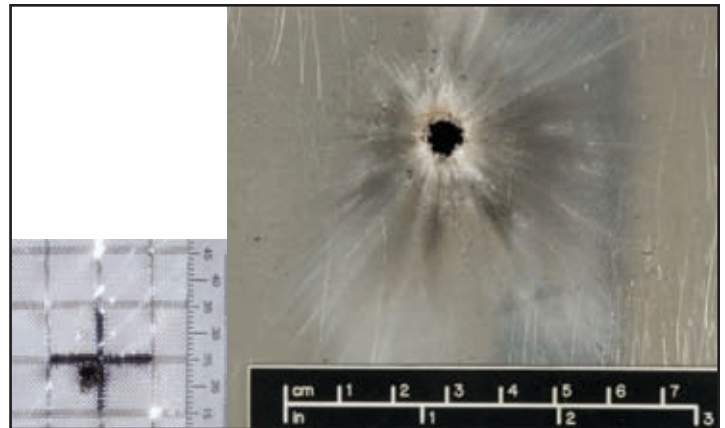


Figure 6. Results from ground test number HITF-7311, for a 0.2 cm aluminum projectile impact at 6.95 km/s and 0 deg. impact angle on a target representative of the FGB compressor shielding. A 0.3 cm hole occurs in the outer thermal blanket cover on the left, and the aluminum honeycomb panel is completely penetrated (1.3 cm hole) on the right. The witness plate behind the honeycomb panel representing the compressor housing was damaged.

Three New Satellite Impact Tests

T. HANADA, K. SAKURABA, AND J.-C. LIOU

Although the current near-Earth orbital debris environment is dominated by explosion fragments, many models predict that more debris will be generated by collisions, rather than explosions, in the future. Therefore, understanding the outcome of both low and hypervelocity satellite impacts is key to modeling the future debris environment. As a first step

to achieve this objective, Kyushu University and the NASA Orbital Debris Program Office have collaborated on a series of impact tests on microsattellites. This article summarizes the three tests completed in early 2007.

The targetsatellitesforthethreenewsatellite impact tests were identical micro satellites, 20 cm by 20 cm by 20 cm in size, slightly larger than those used in the tests conducted in 2005.¹ As shown in Figure 1, the main structure of

each microsattelite was composed of five layers (top and bottom layers and three internal layers parallel to the top and bottom layers) and four side panels. They were assembled by angle bars made of an aluminum alloy and metal spacers. The external layers and side panels were made of Carbon Fiber Reinforced Plastics (CFRP), while the three internal layers were made of Glass Fiber Reinforced Plastics (GFRP). The

continued on page 5

Impact Tests

continued from page 4

interior of each microsatellite was equipped with fully functional electronic devices, such as a wireless radio; lithium-ion batteries; and communication, electric power supply, and command and data handling circuits. The total mass of each microsatellite was approximately 1,300 grams. A special fragment recovery box with a clear acrylic plate window was prepared to hold the target satellite and to observe the fragmentation process. Aluminum alloy solid spheres, each with a diameter of 30 mm and a mass of approximately 40 grams, were prepared as projectiles.

The three satellite impact tests were conducted using the two-stage light gas gun at the Kyushu Institute of Technology, in Kitakyushu, Japan. Table 1 summarizes the impact scenarios. The first and second shots

Table 1. Impact parameters of the three experiments.

Shot	M_t [g]	M_p [g]	V_{imp} [km/s]	E_{imp} / M_t [J/g]	Impact Direction [With Respect to L layers]
1	1,300	39.2	1.66	41.5	Normal
2	1,283	39.2	1.66	42.0	Parallel
3	1,285	39.2	1.72	45.1	Normal

M_t = Target Mass, M_p = Projectile Mass
 V_{imp} = Impact Velocity, E_{imp} = Impact Energy ($= M_p \times V_{imp}^2 / 2$)

time counts in Figure 2 start right at the impact. Some differences in the impact fragmentation can be observed in Figure 2. The third shot produced flame, but the second shot did not. Fragments blew out from the side panels in the third shot, but not in the second shot. This

difference in the impact fragmentation could be caused by impact direction with respect to the inner layers. In the case that the impact direction was normal to the inner layers, the

continued on page 6

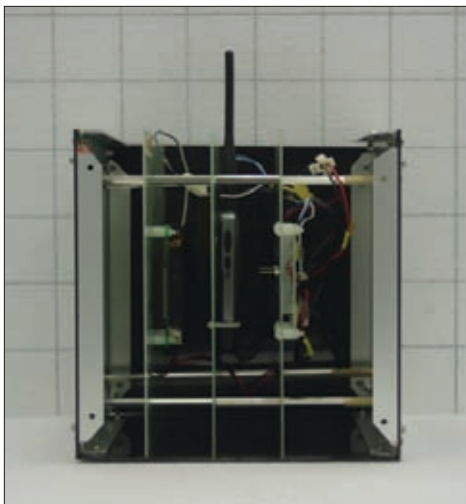


Figure 1. Inside view of the target satellite.

were performed at a speed of 1.66 km/s, whereas the third shot was performed at a speed of 1.72 km/s. Although the first and second shots were performed at the same speed, the impact directions, with respect to the internal layers, were different. The projectile of the first shot impacted perpendicular to the internal layers, whereas the projectile of the second shot impacted parallel to the internal layers. The ratios of impact kinetic energy to target satellite mass for the three tests were 41.5, 42.0, and 45.1 J/g, respectively.

The impact fragmentations of the second and third shots were captured with an ultra-high speed camera in collaboration with the Japan Broadcasting Corporation (NHK in Japanese abbreviation). The impact fragmentation was recorded from two directions; edge-on and diagonally backward. Figure 2 shows the impact fragmentation viewed edge-on. The

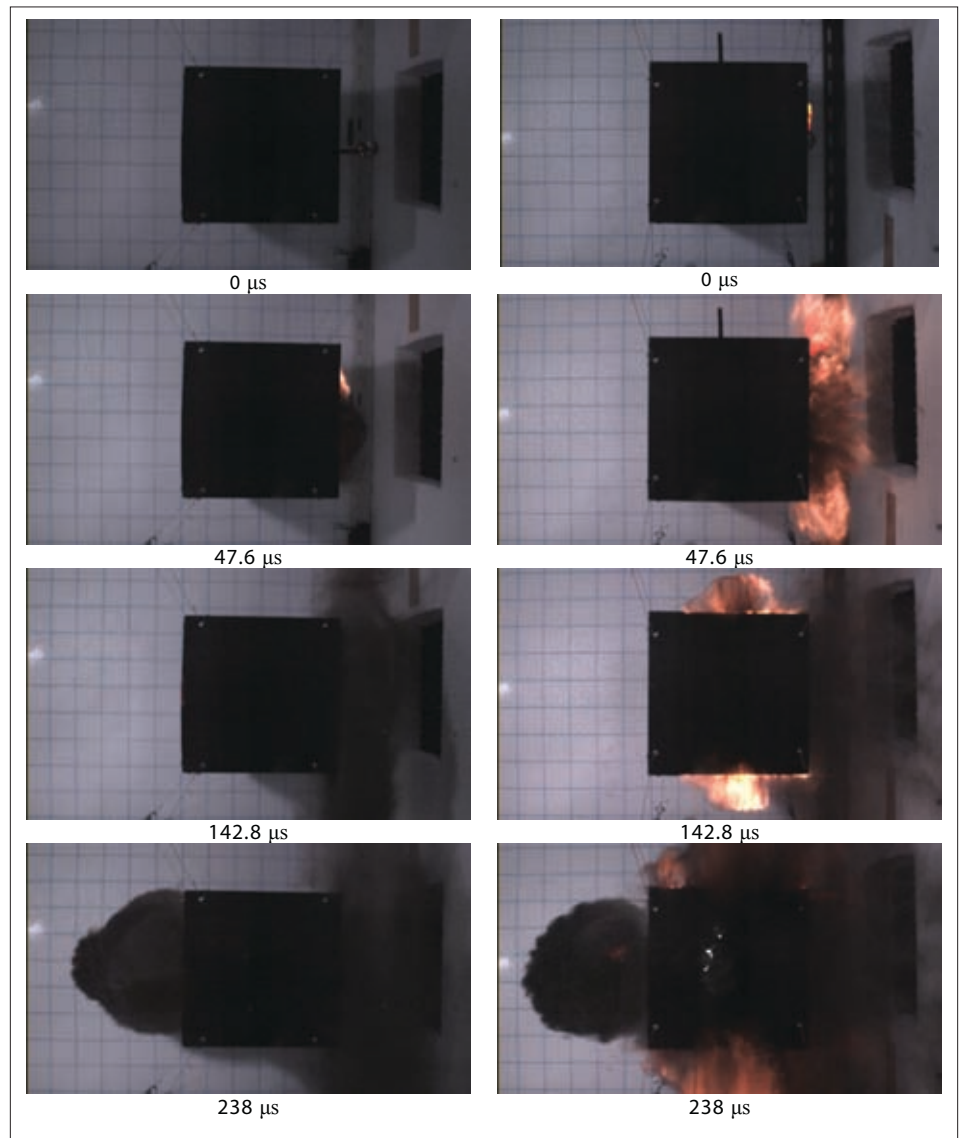


Figure 2. Impact fragmentation of the target satellites: (left) Shot 2; (right) Shot 3.

Impact Tests

continued from page 5

projectile and fragments created by the impact hit the inner layers and created more fragments. In the case that the impact direction was parallel to the inner layers, on the other hand, there were no inner layers for the projectile to hit. In addition, the projectile of the second shot was fragmented before it reached the exterior wall because it impacted the antenna first. This might have also caused the difference in the impact fragmentation.

The NASA standard breakup model defines a collision with a kinetic energy to target mass ratio equal to or greater than 40 J/g to be catastrophic.² The target satellites were completely fragmented in all three tests, consistent with the NASA definition. Figure 3 compares three hundred of the largest fragments from the second and third shots. There is a noticeable difference between the two sets of fragments. Even though the internal layers were separated

from the target satellite, the main box structure still remained intact in the second shot. The other characteristics of the two fragment sets are similar, but the total numbers of fragments for the two sets are quite different. Approximately 1,500 fragments were collected in the third shot, whereas only about 1,000 fragments were collected in the second shot.

The collection of fragments from the first shot is currently in progress. Approximately 1,500 fragments are expected. Once the collection is complete, fragments will be measured and analyzed based on the method used in the NASA standard breakup model.²

Details of these three satellite impact tests and preliminary analysis results will be presented at the 37th COSPAR Scientific Assembly to be held in Montréal, Canada in July 2008.

1. Hanada, T., Tsuruda, Y., and Liou, J.-C., "New Satellite Impact Experiments", *Orbital Debris Quarterly News*, Vol.10, No.3, p.4, 2006.

2. Johnson, N. L., Krisko, P. K., Liou, J.-C., and Anz-Meador, P. D., "NASA's New Breakup Model of EVOLVE 4.0", *Adv. Space Res.*, Vol.28, No.9, pp.1377-1384, 2001. ♦



Figure 3. Three hundred of the largest fragments: (left) Shot 2; (right) Shot 3.

A Preliminary Active Debris Removal Study

J.-C. LIOU AND N. JOHNSON

Concepts for removing large debris from LEO have been proposed for more than 25 years. Early ideas for using the U.S. Space Shuttle, either directly or in conjunction with an orbital transfer vehicle, were found unattractive due to safety, availability, cost, and policy issues. Numerous independent robotic concepts, ranging from classical space-based garbage scoops to momentum and electrodynamic tethers, drag augmentation devices, solar and magnetic sails, and other exotic techniques, have also been considered. However, reviews by panels of international experts have repeatedly failed to identify a single plan which is both technically feasible in the near-term and economically viable.

Nonetheless, in late 2006 the International Academy of Astronautics (IAA) initiated a new study to determine if a nexus of technology, cost, and policy might lead to an achievable means of remediating the near-Earth space environment in the foreseeable future. Although the IAA study will not be completed until late

2008 or 2009, the purpose of the present paper is to describe the potential effectiveness of active debris removal (ADR) operations under various scenarios. These results, in turn, could influence the development of efficient debris removal techniques.

The tool used in the study is the NASA orbital debris evolutionary model LEGEND (a LEO-to-GEO Environment Debris model). A key component of LEGEND is its collision probability estimation module. A removal criterion based upon mass and collision probability, $M \times Pc$, was developed to rank objects at the beginning of each projection year. A pre-defined number of objects with the highest mass and collision probability products were removed from the simulated environment immediately.

Four test scenarios were selected for this case study. The first one was a non-mitigation ("business-as-usual") scenario. The other three scenarios assumed ADR was implemented in the year 2020, with annual debris removal rates of 5, 10, and 20 objects, respectively.

Figure 1 shows the effective numbers of objects, 10 cm and larger, in LEO from the four scenarios. The business-as-usual scenario predicts a fast non-linear growth of the future LEO debris population in the next 200 years. The three ADR scenarios, on the other hand, predict a much slower increase in the environment.

The spatial density distributions of the 10 cm and larger LEO objects are shown in Figure 2. The bottom curve is the environment at the end of 2006. The other four curves, from top to bottom, are the predicted environment in 2206 from the non-mitigation, ADR 2020/5, ADR 2020/10, and ADR 2020/20 scenarios, respectively. It is very clear that active debris removal, based on the selection criterion described earlier, is a very effective means to limit the population growth in high collision activity regions between 800 and 1000 km.

One possible modification to improve the selection criterion of $M \times Pc$ is to include the longevity factor. When two objects

continued on page 7

Debris Removal

continued from page 6

have similar $M \times P_c$ values, it is obvious that removing the object which has a longer orbital lifetime would have a more positive impact on the environment. The difficulty here is how to properly incorporate the lifetime dependence into the equation. Since orbital lifetime does not increase linearly with increasing altitude, a linear dependence of orbital lifetime incorporated into $M \times P_c$ may result in the removal of all objects at higher altitudes, e.g., 1500 km, before any objects at lower altitudes are considered. The present study only addressed the near-term (i.e., next

200 years or so) environment concerns. ADR scenarios based on the selection criterion of $M \times P_c$ effectively reduce the population in regions which have the greatest potential of growth in 200 years (see Figure 2). If the objective is to address the population growth over a much longer period of time, e.g., thousands of years, the direct implementation of orbital lifetime into the selection criterion may be further justified.

The actual implementation of any mitigation measures to remove objects from space is very complicated. The cost and technical

challenges are the two major obstacles that will not be resolved in the near future. Additional issues, such as ownership, liability, and policy, need to be addressed as well. However, if the mitigation measures currently adopted by international space agencies and industry are insufficient to limit the growth of the future debris population, effective active debris removal, such as the one based on the strategy described here, must be seriously considered as an option to preserve the near-Earth space for future generations. ♦

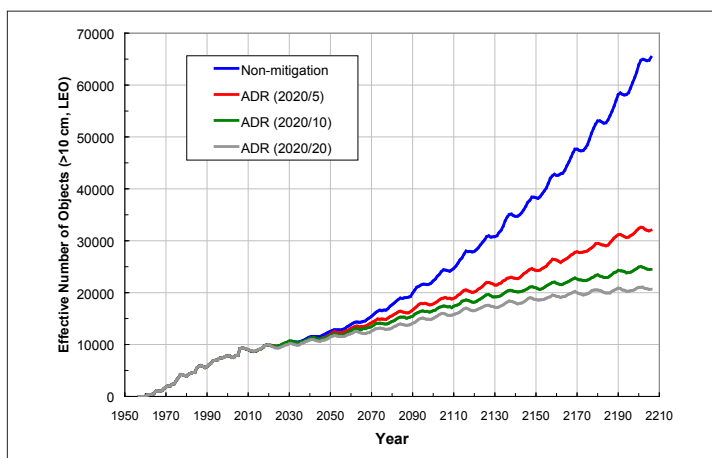


Figure 1. LEGEND-simulated LEO debris populations (objects 10 cm and larger) between 1957 and 2006 (historical), and between 2007 and 2206 (future projection). Each curve represented the average of 100 Monte Carlo runs.

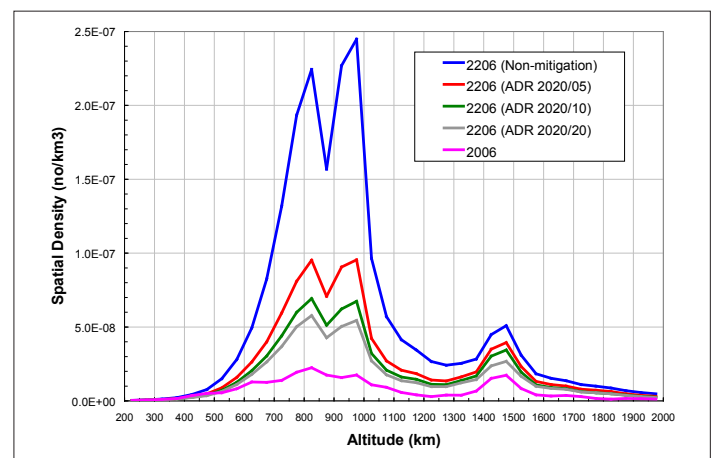


Figure 2. Spatial density distribution of objects 10 cm and larger in LEO. The bottom curve represents the LEO environment at the end of 2006. The other four curves, from top to bottom, are the predicted environment in 2206 from the non-mitigation, ADR 2020/5, ADR 2020/10, and ADR 2020/20 scenarios.

ABSTRACTS FROM THE NASA ORBITAL DEBRIS PROGRAM OFFICE

8th Air Force Maui Optical and Supercomputing (AMOS) Technical Conference
10-14 September 2007, Wailea, Maui, Hawaii, USA

Remote and Ground Truth Spectral Measurement Comparisons

K. ABERCROMBY, K. HAMADA, M. GUYOTE, J. OKADA, AND E. BARKER

FORMOSAT III are a set of six research satellites from Taiwan that were launched in April 2006. The satellites are in 800 km, 71 degree inclination orbits and separated by 24 degrees in ascending node. Ground truth spectral measurements were taken of outer surface materials on FORMOSAT III. From those measurements, a computer model was built to predict the spectral reflectance, which included phase angle and orientation of the spacecraft relative to the observer. However,

materials exposed to the space environment have exhibited spectral changes including a darkening and a “reddening” of the spectra. This “reddening” was seen as an increase in slope of the reflectance as the wavelength increases. Therefore, the model of pristine materials was augmented to include the space weathering effects.

Remote data were collected on two of the six FORMOSAT satellites using the 1.6 meter telescope at AMOS (Air Force Maui Optical and Supercomputing) site with the Spica spectrometer. Due to the separation

in ascending node, observations were made on whichever one of the six satellites was visible on that specific night. Three nights of data were collected using the red (6000-9500 angstroms) filter and two nights of data were collected using the blue (3200-6600 angstroms) filter. A comparison of the data showed a good match to the pristine model for the blue filter region. The absorption feature near 5500 angstroms due to the copper-colored Kapton multi-layer insulation was very apparent in the remote samples and a good fit to the data was seen in both satellites

continued on page 8

Remote and Ground Truth

continued from page 7

observed. The features in the red filter regime agreed with the pristine model up through 7000 angstroms where the reddening begins and the slope of the remote sample increases. A comparison of the two satellites showed similar features in the red and blue filter regions, i.e., the satellites were aging at the same rate.

A comparison of the pristine model to the first month of remote measurements showed the amount by which the satellite had reddened. This information was used in the space weathered model to predict the second month's reflectance measurement. The results showed that the reddening did not increase

from the first month of observations to the second. A third month of data will be necessary to determine if the reddening occurs instantly and then stabilizes with time or if the effect continues to increase with time. ♦

An Attempt to Observe Debris from the Breakup of a Titan 3C-4 Transtage

E. BARKER, M. MATNEY, T. YANAGISAWA, AND P. SEITZER

In February 2007, dedicated observations were made of the orbital space predicted to contain debris from the breakup of the Titan 3C-4 transtage back on 21 February 1992. These observations were carried out on the Michigan Orbital DEbris Survey Telescope (MODEST) in Chile with its 1.3° field of view. The search region or orbital space (inclination and right ascension of the ascending node (RAAN) was predicted using NASA's LEGEND (LEO-to-GEO Environment Debris) code to generate a Titan debris cloud. Breakup fragments are created based on the NASA Standard Breakup Model (including fragment size, area-to-mass (A/m), and delta-V distributions). Once fragments are created, they are propagated forward in time with a subroutine GEOPROP. Perturbations included in GEOPROP are those due to solar/lunar gravity, radiation pressure, and major geopotential terms. Barker, et. al, (*Proceedings of AMOS 2006 Technical Conference*, pp. 596-604) used similar LEGEND predictions to correlate survey observations made by MODEST in February 2002 and found several possible

night-to-night correlations in the limited survey dataset.

One conclusion of the February 2002 survey search was to dedicate a MODEST run to observing a GEO region predicted to contain debris fragments and actual Titan debris objects (SSN 25000, 25001, and 30000). Such a dedicated run was undertaken with MODEST between the 17 and 23 of February 2007 (UT dates). MODEST's limiting magnitude of 18.0 (S/N~10) corresponds to a size of 22 cm assuming a diffuse Lambertian albedo of 0.2. However, based on observed breakup data, we expect most debris fragments to be smaller than 22 cm, which implies a need to increase the effective sensitivity of MODEST for smaller objects. MODEST's limiting size could not be lowered by increasing the exposure time from 5 to 20 seconds due to trailing of the image. However, special image processing did allow the detection of smaller debris. Special processing combined several individual CCD images to detect faint objects that were invisible on a single CCD image. Sub-images are cropped from six consecutive CCD images with pixel shifts between images being consistent with the predicted movement

of a Titan object. A median image of all the sub-images is then created, leaving only those objects with the proper Titan motion. Limiting the median image in this manner brings the needed computer time to process all images taken on one night down to about 50 hours of CPU time.

Successful observations were carried out over six consecutive nights. Positions for each of the 62 detected targets on individual nights were fit under the assumption of circular orbits (ACO). Those targets that were observed on other nights and that had similar ACO orbital parameters were combined and their observed positions fit to a full six-parameter orbit. Combinations of targets having RMS fits less than ~10 arcseconds were considered to be the same target. Six combinations were correlated to cataloged targets (CTs). Cataloged Titan debris (SSNs 25000, 25001, 30000) were not detected because they were not observable during nighttime hours. Nine combinations could not be correlated to cataloged targets, hence they were defined as UCTs. These UCTs have orbital elements very similar to those predicted by LEGEND and thus are strong candidates for Titan debris. ♦

Derivation and Application of a Global Albedo Yielding an Optical Brightness to Physical Size Transformation Free of Systematic Errors

M. MULROONEY, M. MATNEY

We have developed a technique for estimating the intrinsic size distribution of orbital debris objects via optical measurements alone. The process is predicated on apriori knowledge of the power-law size distribution of debris (as indicated by radar RCS measurements) and the log-normal distribution of optical albedos. Since the observed distribution of optical brightness is the convolution of the parent (size) population with the albedo distribution, it is a straightforward matter to transform a given distribution of optical brightness back to a size distribution by the appropriate choice of a single albedo value. This is true because

the integration of a power-law with a log-normal distribution yields a Gaussian-blurred power law distribution with identical power-law exponent. Application of a single albedo to this distribution recovers a simple power-law that is linearly offset from the original distribution by a constant whose value depends on the choice of the albedo. Significantly, there exists a unique "weighted-average" albedo, which, when applied to an observed brightness distribution, yields zero offset and therefore recovers the original size distribution. For physically realistic power-laws of negative slope, the proper choice of weighted albedo effectively removes the biases caused by the large number of small

objects that look anomalously "large" (bright) and the lower number of large objects looking anomalously "small" (dim).

Based on this comprehensive analysis, a global value of 0.13 should be applied to all orbital debris albedo-based, brightness-to-size transformations of debris objects, regardless of data source. This represents a modification to the canonical value of 0.1 widely employed. Herein we present the empirical and mathematical arguments for this approach and by example, apply it to a comprehensive set of photometric data acquired via NASA's Liquid Mirror Telescopes during the 2000 observing season. ♦

Optical Properties of Multi-Layered Insulation

H. RODRIGUEZ, K. ABERCROMBY, M. MULROONEY, AND E. BARKER

Multi-layer insulation (MLI) is a material used on rocket bodies and satellites primarily for thermal insulation. MLI is comprised of a variety of materials, layer numbers, and dimensions to satisfy specific design requirements. Typically, it is a sandwich of outward-facing, copper-colored Kapton layers with inward-facing, aluminized backing. The inner layers consist of alternating DACRON or Nomex netting and aluminized Mylar. From an orbital mechanics perspective, if this material becomes separated from a spacecraft or rocket body, its orbit will vary greatly in eccentricity due to both its high area-to-mass ratio (A/m) and its susceptibility to solar radiation pressure perturbations. Recently, a debris population was found with high A/m that could be MLI.

Laboratory photometric measurements of one intact piece and three different layers of MLI are presented in an effort to ascertain the characteristics of MLI light curves and aid in

identifying the source of the new population. For this paper, the layers used will be consistent with the aforementioned common MLI. Using a robotic arm, the piece was rotated from zero to 360 degrees in 10 degree increments along the object's longest axis. Laboratory photometric data was recorded with a CCD camera and a 300 W Xenon arc light source selected to approximate the solar spectrum. The measurements were taken in white light and using various filters [Johnson Blue (B), Visible (V), and Bessell Red (R)], all taken at an 18 degree (light-object-camera) phase angle selected to closely match typical GEO observations that follow the anti-solar point. As expected, the MLI pieces exhibited characteristics similar to a bimodal magnitude plot of a flat plate, but with photometric features dependent upon the layer composition. To minimize highlight saturation (and consequent loss of intensity information), exposure times were selected empirically based on layer type and filter.

In addition to photometric laboratory measurements, laboratory spectral measure-

ments were acquired for each MLI sample. Spectral data will be combined to match the wavelength region of photometric data to establish a fiduciary reference for the photometric measurements. Not only will this help validate the color photometry, but it will also assist interpretation and analysis of telescopic data. As an example, copper-colored Kapton shows a strong absorption feature near 4800 angstroms. If the observed debris is MLI and the outer layer of copper coloring of Kapton is present, evidence of this material should be seen spectroscopically by the specific absorption feature as well as photometrically (e.g., by using R-B (red-blue) light curves).

Using laboratory photometric and spectroscopic measurements, an optical property database is provided for a representative high A/m object. These results should directly aid the accurate interpretation of telescopically acquired optical orbital debris photometry of both high A/m targets as well as satellites and spacecraft that incorporate MLI. ♦

Optical Studies of Space Debris at GEO – Survey and Follow-up with Two Telescopes

P. SEITZER, K. ABERCROMBY, E. BARKER, AND H. RODRIGUEZ

For 14 nights in March 2007, we used two telescopes at the Cerro Tololo Inter-American Observatory (CTIO) in Chile to study the nature of space debris at Geosynchronous Earth Orbit (GEO).

In this project, one telescope was dedicated to survey operations, while a second telescope was used for follow-up observations for orbits and colors. The goal was to obtain orbital and photometric information on every faint object found with the survey telescope. Thus we concentrate on objects fainter than $R = 15$ th magnitude.

MODEST (Michigan Orbital DEbris Survey Telescope, the University of Michigan's 0.6/0.9-m Schmidt telescope at CTIO) was used in survey mode every night to scan a

strip of sky 1.3-deg wide in declination by over 100 degrees long in hour angle. Five-second exposures were obtained every 37.9 seconds, reaching a limiting R magnitude of 18.0 for a S/N of 10. With a field-of-view (FOV) of 1.3-degrees, an average of eight detections are made of an individual object at GEO during a 5.2 minute timespan.

A real-time processing pipeline detects objects and provides positions and magnitudes to the CTIO 0.9-m equipped with CCD imager with a FOV of 0.22 degree. Predictions of future rates and positions for the first recovery observation with the 0.9-m were made by fitting an assumed circular orbit to the observed MODEST positions.

The recovery rate with the 0.9-m of objects found by MODEST was over 85%. The average time between the last detection

on MODEST and acquisition on the 0.9-m was 17 minutes. The quickest hand-over was 4 minutes.

The 0.9-m was used to determine:

1. Full six-parameter orbits (including eccentricity). An initial orbit was determined based on observations during one night, and then refined with observations on subsequent nights. One challenge of studying these objects with periods close to 23h56m is that frequent observations are required to refine and update the orbit so the object can be recovered later.

2. Magnitudes and colors in the standard astronomical BVRI system. Sequences of 10 observations in each filter were obtained to measure brightness variations.

In this paper we will summarize the results obtained and outline future work. ♦

58th International Astronautical Conference 24-28 September 2007, Hyderabad, India

An Analysis of the Orbital Distribution of Solid Rocket Motor Slag

M. HORSTMAN

The contribution made by orbiting solid rocket motors (SRMs) to the orbital debris environment is both potentially significant and insufficiently studied. A combination of rocket

motor design and the mechanisms of the combustion process can lead to the emission of sufficiently large and numerous by-products to warrant assessment of their contribution to the orbital debris environment. These

particles are believed formed during SRM tail-off by the rapid expansion, dissemination, and solidification of the molten Al_2O_3 slag pool accumulated during the main burn phase of SRMs utilizing immersion-type nozzles.

Analysis of the Orbital Distribution

continued from page 9

Though the usage of SRMs is low compared to the usage of liquid-fueled motors, the propensity of SRMs to generate particles in the 100 micron and larger size regime leads to concerns about such additional mass contributing to the debris environment. Particle sizes as large as one centimeter have been witnessed in ground tests conducted under vacuum conditions and comparable sizes have been estimated via ground-based telescopic and

in-situ observations of sub-orbital SRM tail-off events.

Using such sub-orbital and post recovery observations, a simplistic number-size-velocity distribution of slag from on-orbit SRM firings was postulated (Mulrooney 2007). In this paper we have developed more elaborate distributions and emission scenarios and modeled the resultant orbital population and its time evolution by incorporating a historical

database of SRM launches, propellant masses, and likely location and time of particulate deposition. From this analysis, a more comprehensive understanding has been obtained of the role of SRM ejecta in the orbital debris environment, indicating that SRM slag is a significant component of the current and future population. ♦

The Characteristics and Consequences of the Break-up of the Fengyun-1C Spacecraft

N. JOHNSON, E. STANSBERY, J.-C. LIOU, C. STOKELY, AND D. WHITLOCK

The intentional break-up of the Fengyun-1C spacecraft on 11 January 2007 via hypervelocity collision with a ballistic object created the most severe artificial debris cloud in Earth orbit since the beginning of space exploration. More than 2000 debris on the order of 10 cm or greater in size have been identified by the U.S. Space Surveillance Network. The majority of these debris reside

in long-lived orbits. The NASA Orbital Debris Program Office has conducted a thorough examination of the nature of the Fengyun-1C debris cloud, using SSN data for larger debris and special Haystack radar observations for smaller debris. These data have been compared with the NASA standard satellite break-up model for collisions, and the results are presented in this paper. The orbital longevity of the debris has also been evaluated for both small and large debris. The consequent long-term spatial

density effects on the low Earth orbit regime are then described. Finally, collision probabilities between the Fengyun-1C debris cloud and the resident space object population of 1 January 2007 have been calculated. The potential effect on the growth of the near-Earth satellite population is presented. ♦

A Sensitivity Study of the Effectiveness of Active Debris Removal in LEO

J-C LIOU, N. JOHNSON

The near-Earth orbital debris population will continue to increase in the future due to ongoing space activities, on-orbit explosions, and accidental collisions among resident space objects. Commonly adopted mitigation measures, such as limiting postmission orbital lifetimes of satellites to less than 25 years, will slow down the population growth, but may be insufficient to stabilize the environment.

The nature of the growth, in the low Earth orbit (LEO) region, is further demonstrated by a recent study where no future space launches were conducted in the environment projection

simulations. The results indicate that, even with no new launches, the LEO debris population would remain relatively constant for only the next 50 years. Beyond that, the debris population would begin to increase noticeably, due to the production of collisional debris.

Therefore, to better limit the growth of future debris population to protect the environment, remediation options, i.e., removing existing large and massive objects from orbit, need to be considered. This paper does not intend to address the technical or economical issues for active debris removal. Rather, the objective is to provide a sensitivity

study to quantify the effectiveness of various remediation options. A removal criterion based upon mass and collision probability is developed to rank objects at the beginning of each projection year. This study includes simulations with removal rates ranging from 5 to 20 objects per year, starting in the year 2020. The outcome of each simulation is analyzed and compared with others. The summary of the study serves as a general guideline for future debris removal consideration. ♦

Improvements to NASA's Debris Assessment Software

J. OPIELA, N. JOHNSON

NASA's Debris Assessment Software (DAS) has been substantially revised and expanded. DAS is designed to assist NASA programs in performing orbital debris assessments, as described in NASA's "Guidelines and Assessment Procedures for Limiting Orbital Debris." The extensive upgrade of DAS was undertaken to reflect changes in the debris mitigation guidelines, to incorporate recommendations from DAS users, and to take advantage of recent software capabilities for greater user utility.

DAS 2.0 includes an updated environment model and enhanced orbital propagators and reentry-survivability models. The ORDEM96

debris environment model has been replaced by ORDEM2000 in DAS 2.0. The new DAS is also designed to accept anticipated revisions to the debris environment definition. Numerous upgrades have also been applied to the assessment of human casualty potential due to reentering debris.

Routines derived from the Object Reentry Survival Analysis Tool, Version 6.0 (ORSAT 6.0), determine which objects are assessed to survive reentry, and the resulting risk of human casualty is calculated directly based upon the orbital inclination and a future world population database. When evaluating reentry risks, the user may enter up to 200 unique hardware components for each launched object,

in up to four nested levels. This latter feature allows the software to model more accurately components that are exposed below the initial breakup altitude.

The new DAS 2.0 provides an updated set of tools for users to assess their mission's compliance with the NASA Safety Standard and does so with a clear and easy-to-understand interface. The new native Microsoft Windows graphical user interface (GUI) is a vast improvement over the previous DOS-based interface. In the new version, the layout of functions is clear, and the GUI includes the standard Windows-style "Help" functions. The underlying routines within the DAS code are also improved. ♦

On the Determination of Poisson Statistics for Haystack Radar Observations of Orbital Debris

C. STOKELY, J. BENBROOK, AND M. HORSTMAN

A convenient and powerful method is used to determine if radar detections of orbital debris are observed independently with some average rate, as given by Poisson statistics. This is done by analyzing the time interval between detection events. For Poisson statistics the time interval between events is an exponential distribution. This distribution is a

special case of the Erlang distribution that is used in estimating traffic loads on telephone networks. Poisson statistics form the basis of many orbital debris models, but the statistical basis of these models have not been empirically demonstrated until now. Interestingly, during the fiscal year 2003 observations with the Haystack radar in a fixed staring mode, there are no deviations observed from that expected by Poisson statistics. Furthermore, the results

are independent of altitude and inclination. One would potentially expect some significant clustering of events in time as a result of satellite breakups but the Poisson nature of the time distribution indicates that such debris disperse rapidly enough in time to appear uncorrelated in observations. ♦

Strategy for Detection of Eccentric Objects Near the Geosynchronous Region

T. YANAGISAWA

Detection of eccentric objects with an orbital period near 24 hours is a very important issue. However, the extremely narrow fields-of-view of optical telescopes hinder us from identifying eccentric objects. A new observation strategy to systematically detect these objects and determine their orbits precisely with one telescope is outlined in this presentation. Basically, one specific geosynchronous (GEO) location (not one specific celestial position) is observed on two nights. Objects which pass through that location in the first night must pass through that location again in the second night. By identifying the same objects from two nights of data, rough orbits for those objects are determined. A third night is needed for precise orbital determination.

The current observation strategy for NASA is to observe a few celestial positions for one night and detect as many objects (in, near, or crossing GEO) as possible. These objects have different motions from the celestial motion, which limits the observable time for each object to about five minutes. From a five-minute orbital arc, it is difficult to determine the precise orbit of an object. Therefore, circular orbits are assumed for all detections. This assumption makes it possible to calculate their semi-major axes, inclinations, and the right ascensions of ascending node (RAAN). Various applications, such as the average distributions of GEO objects and identifications of some groups in the RAAN-inclination phase space, are possible using these data. More precise orbit determinations

are needed for other applications, such as long-term tracking and impact hazard analysis. A reliable orbital determination requires at least three observations to create a long arc. However, the narrow fields-of-view of optical telescopes makes it difficult to re-acquire the same objects after a few hours, especially in the case of eccentric orbits. To get a long arc, a telescope has to follow one target for a long period of time. Determining the precise orbits of many GEO-crossing objects demands a lot of time and is not an efficient use of telescope time. The proposed new observation strategy has the ability to cope with this situation to determine precise orbital elements of many objects in relatively short observation time. An application of this strategy to the observation for Titan fragments is also discussed. ♦

MEETING REPORTS

8th Air Force Maui Optical and Supercomputing (AMOS) Technical Conference 10-14 September 2007, Wailea, Maui, Hawaii, USA

The 2005 Advanced Maui Optical and Space Surveillance Technologies Conference was conducted from 12 - 15 September 2007 in Wailea, Maui. More than 600 participants interested in all aspects of space surveillance attended the conference. Thomas Schildknecht chaired the orbital debris session, which consisted of several papers and posters. The highlights are shown here:

Atsushi Nakejima, from the Japan Aerospace Exploration Agency, discussed the status of space debris observations in Japan. His talk gave an overview of the systems, status, and

regions of interest for the JAXA program. Pat Seitzer, from the University of Michigan, gave a talk on the two-telescope system in Chile used for survey and follow-up debris studies. The program has been very successful. Ed Barker, from NASA JSC, spoke about the observations of debris that appear to originate from the Titan 3C-4 Transtage breakup. The data was taken at the Cerro Tololo Inter-American Observatory in Chile. Thomas Schildknecht, from the University of Bern, discussed the progress of the study of the recently discovered high area-to-mass ratio debris. Matt Hejduk,

from RABA technologies, gave the final talk of the session regarding the phase functions of deep-space orbital debris. Heather Rodriguez, ESCG/Jacobs, had a poster that showed the progress of determining the optical properties of multi-layer insulation (MLI). MLI is one of the possibilities for the origin of the high area-to-mass objects. Another poster was presented by Mark Mulrooney, from ESCG/MEI, which discussed the use of a global albedo to obtain an optical brightness to physical size transformation free of systematic errors. ♦

58th International Astronautical Conference 24-28 September 2007, Hyderabad, India

The Space Debris Symposium at the 58th International Astronautical Congress took place in Hyderabad, India, during the week of 24 - 28 September. A total of 21 oral and 5 poster papers were presented. In the measurement session, several papers highlighted the recent optical and radar measurements conducted by the French Space Agency, the European Space

Agency, the Italian Space Agency, NASA, and ROSCOSMOS. Papers presented in the modeling session included LEO and GEO environment modeling efforts by ESA, the Indian Space Research Organisation, the Japan Aerospace Exploration Agency, and NASA. Additional presentations on the characterization of the Fengyun-1C breakup, active debris

removal, and mitigation models were given in other sessions. Several papers addressing the legal aspects of orbital debris were also presented in the International Colloquium on the Law of Outer Space sessions during the Congress. ♦

INTERNATIONAL SPACE MISSIONS

01 July – 30 September 2007

International Designator	Payloads	Country/ Organization	Perigee (KM)	Apogee (KM)	Inclination (DEG)	Earth Orbital Rocket Bodies	Other Cataloged Debris
2007-030A	SAR LUPE 2	GERMANY	473	498	98.2	1	0
2007-031A	CHINASAT 6B	CHINA	35776	35797	0.0	1	0
2007-032A	DIRECTV 10	USA	35781	35792	0.1	1	1
2007-033A	PROGRESS-M 61	RUSSIA	342	346	51.6	1	0
2007-034A	PHOENIX	USA	HELIOCENTRIC			1	0
2007-035A	STS-118	USA	337	348	51.6	0	0
2007-036A	SPACEWAY 3	USA	29036	42563	0.2	1	1
2007-036B	BSAT 3A	JAPAN	35777	35798	0.0		
2007-037A	INSAT 4CR	INDIA	35773	35799	0.1	1	0
2007-038A	COSMOS 2429	RUSSIA	955	1010	83.0	1	0
2007-039A	SELENE (KAGUYA)	JAPAN	LUNAR ORBIT			0	0
2007-039B	RSAT	JAPAN	LUNAR ORBIT				
2007-039C	VRAD	JAPAN	LUNAR ORBIT				
2007-040A	FOTON M-3	RUSSIA	258	280	62.9	1	3
2007-041A	WORLDVIEW 1	USA	493	495	97.5	1	0
2007-042A	CBERS 2B	CHINA/BRAZIL	773	774	98.6	1	0
2007-043A	DAWN	USA	HELIOCENTRIC			1	0

ORBITAL BOX SCORE

(as of 03 October 2007 as cataloged by US SPACE SURVEILLANCE NETWORK)

Country	Payloads	Rocket Bodies & Debris	Total
CHINA	63	2568	2631
CIS	1361	2949	4310
ESA	37	36	73
FRANCE	45	317	362
INDIA	34	107	141
JAPAN	102	70	172
US	1073	3115	4188
OTHER	386	88	474
TOTAL	3101	9250	12351

Technical Editor

J.-C. Liou

Managing Editor

Debi Shoots



Correspondence concerning the ODQN can be sent to:

Debi Shoots

NASA Johnson Space Center

Orbital Debris Program Office

Mail Code JE104

Houston, TX 77058



debra.d.shoots@nasa.gov

UPCOMING MEETING

13-20 July 2008: The 37th COSPAR Scientific Assembly, Montréal, Canada.

Three debris sessions are planned for the conference. They will address advances in ground-based and in-situ measurement techniques; debris and meteoroid environment models and related collision risk estimates for space missions; on-orbit collision avoidance; re-entry risk assessments; debris mitigation measures and their effectiveness for long-term environment stability; national and international debris mitigation standards and guidelines; hypervelocity impact technologies; and on-orbit shielding concepts. The abstract submission deadline is 17 February 2008. Additional information for the conference is available at <http://www.cospar2008.org/index.html>.

HOW TO SUBSCRIBE...

To receive email notification when the latest newsletter is available, please fill out the ODQN Subscription Request Form located on the NASA Orbital Debris Program Office website, www.orbitaldebris.jsc.nasa.gov. This form can be accessed by clicking on "Quarterly News" in the Quick Links area of the website and selecting "ODQN Subscription" from the pop-up box that appears.



National Aeronautics and Space Administration

Lyndon B. Johnson Space Center
2101 NASA Parkway
Houston, TX 77058

www.nasa.gov